PROCEEDINGS OF SCIENCE

Searching for air showers with RNO-G

Jakob Henrichs[a,b,*] **for the RNO-G Collaboration**

(a complete list of authors can be found at the end of the proceedings)

[a] *DESY, Platanenallee 6, 15738, Zeuthen, Germany*

[b] *Erlangen Center for Astroparticle Physics (ECAP), Friedrich-Alexander-University Erlangen-Nuremberg, 91058 Erlangen, Germany*

E-mail: jakob.henrichs@desy.de

The Radio Neutrino Observatory – Greenland (RNO-G) is an in-ice neutrino detector, using radio emission to target the first measurement of neutrinos beyond PeV energies. In total 35 stations are planned for the detector, resulting in a detection volume of around 100 km^3. Each of these stations is equipped with deep antennas embedded $\sim$ 100 m into the ice and downward-pointing log-periodic dipole antennas (LPDA) buried $\sim$ 3 m into the snow. At each station, three additional buried LPDA are pointing towards the sky and thus can be used to look for cosmic-ray induced air-showers. These air showers are a background for the RNO-G detector and therefore important to understand, but they also can be used as a calibration tool. In order to find the air-shower signals, we apply an analysis based on template matching to the data.

We present the current status of the analysis targeting the detection of cosmic-rays induced air showers. This includes the presentation of a method to create a complete template set and a first look at RNO-G data.

9th International Workshop on Acoustic and Radio EeV Neutrino Detection Activities - ARENA2022
7-10 June 2022
Santiago de Compostela, Spain

*Speaker

PoS(ARENA2022)007

1. Radio Neutrino Observatory Greenland (RNO-G)

The Radio Neutrino Observatory Greenland [1] is an in-ice neutrino detector, which is currently under construction and is located at Summit Station, Greenland. The goal of the detector is the detection of astrophysical and cosmogenic neutrinos above PeV energies. Additionally, RNO-G is a pathfinder to help inform the planned radio array of IceCube-Gen2 [2]. When ultra-high energy neutrinos interact in the ice, they produce particle showers, which create radio emission mainly via the Askaryan effect [3]. The resulting radio emission can be measured and used to reconstruct the energy and direction of the neutrinos [4, 5]. At these high energies, a large detection volume is needed to measure neutrinos. Thus radio emission is the preferred detection method, because due to the larger attenuation length a larger effective volume can be reached with fewer instrumentation compared to optical neutrino telescopes. For RNO-G, in total 35 independent stations, with a grid spacing of 1.25 km are planned, resulting in a total detection volume of around 100 km^3 of ice. The construction started in July 2021 and since August 2022 seven stations are installed and operating. Each of the stations is equipped with 24 antennas. A drawing of a single station can be found in Figure 1a. The station can be separated into a deep and a shallow component. The deep component consists of 15 antennas (4 horizontally polarized (Hpol), 11 vertically polarized (Vpol)) grouped into three strings, reaching a depth of ∼100 m. Both antenna types are necessary to achieve a good direction reconstruction. The shallow component consists of 9 Log-Periodic Dipole Antennas (LPDA), which are buried into the snow at a depth of ∼3 m. Six of the LPDAs are pointing downward and thus can be used for neutrino detection. The other three LPDAs are pointing towards the sky and can be used to measure and tag background from above. The upward facing antennas will be used in the following to find cosmic-ray induced air-showers candidates.

2. Backgrounds

The backgrounds can be grouped into two classes, physical and anthropogenic origin. In the latter category falls noise created by e.g. radio communication and snow mobiles driving by. A possible background of the first category is coming from events created by the triboelectric effect during high wind periods [6]. The other backgrounds of this category are connected to cosmic rays. When an ultra-high energetic cosmic ray (UHECR) hit the atmosphere, a particle air shower is created. This particle shower produces radio emission via the Askaryan and dominantly via the geomagnetic emission [7, 8]. The resulting radio emission can be measured and can act as a possible background to neutrino detection. In addition, high energetic muons are created inside the particle showers and can interact in the ice and yield large localized energy losses, creating particle showers and thus radio emission [9]. As RNO-G is located at an altitude of ∼ 3000 m a particle air-shower with a small zenith angle can hit the ice before it is fully developed. In this case, the particle shower further develops in the ice, creating radio emission [10]. Finally, all the created radio emission described above can be reflected by reflective layers in the ice [11]. The analysis, presented in this work, aims at the detection of the direct radio emission of air showers. The possibility to detect air showers can be used to tag these events and to better understand the background and the detector. Due to the similarity of the air shower signal to a potential neutrino signal (both are bipolar and only of a few nanosecond length), the air showers can be used to test the complete detection chain under

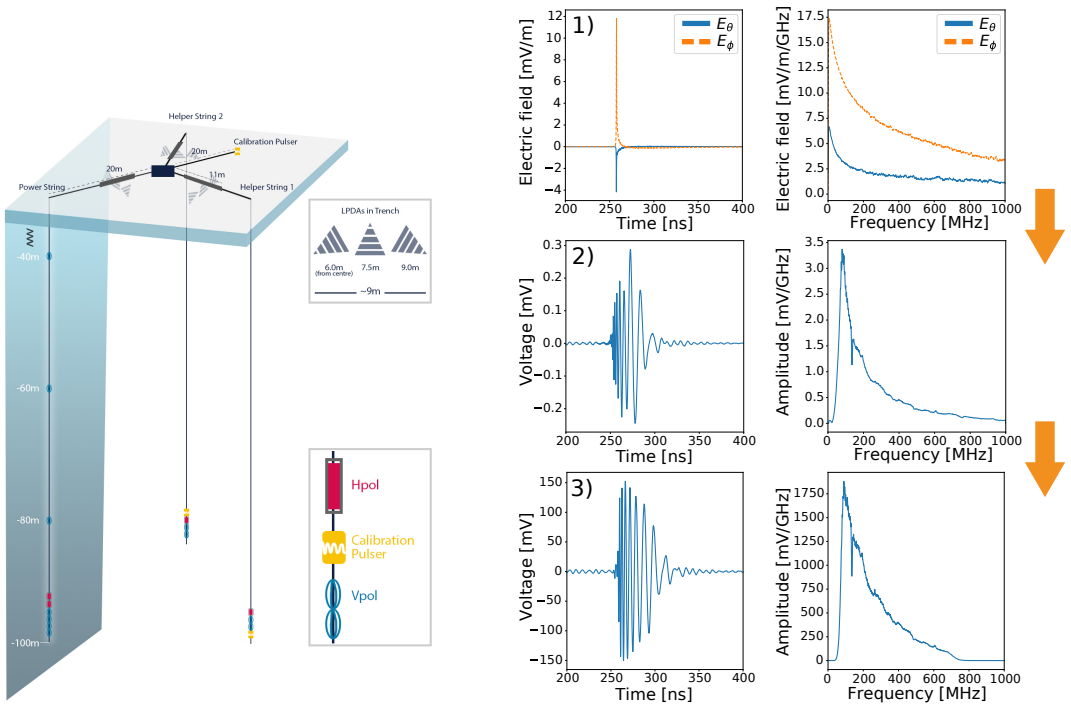

(a) **(b)**

Figure 1: a): A drawing of an RNO-G station with all 24 antennas and the calibration pulsers. **b):** 1) The left panel shows the time domain of a simulated cosmic ray signal, while the right panel shows the corresponding frequency domain. 2) The plots show the signal after the LPDA, but before going into the amplifier and trigger logic. 3) The plots show the signal how it looks for the trigger and how it is saved (in ADC).

realistic conditions. A simulated cosmic ray signal and what it looks like after running through the electronic chain can be found in Figure 1b. Moreover, the signals can be used for an in-situ calibration and to increase confidence in the reconstruction algorithms.

3. Cosmic-ray analysis

In the following, we will introduce the strategy of the cosmic-ray analysis and present the current status. In the end, we will show a first look at the data, by applying the analysis to data from two stations.

3.1 General strategy

For the analysis, the general strategy is to use template matching, meaning that the data is correlated with templates of cosmic-rays waveforms. Noise events, correlated with the templates, should give a rather small correlation value, while cosmic-ray events should give a high correlation value. The correlation value is a measure for the agreement of the data with the compared template (see Equation 1) As a result, the correlation value can be used to discriminate noise from signal events. A similar analysis was used by the ARIANNA collaboration for their cosmic-ray analysis and was successful [12]. For the analysis done by ARIANNA, the templates were created by using the waveforms from cosmic-rays simulations. However, they did not exploit the similarities

of different simulations and thus had numerous templates (~ 200,000), which is computationally expensive, in particular for a steadily increasing data-set. Additionally, the RNO-G waveforms (2048 samples) are longer than the ARIANNA waveforms (256 samples) [12]. For the RNO-G analysis, the first step is to create a template set which covers the parameter space completely. By using the similarities of the different signals, a smaller template set will be created. Using the template set a correlation value can be calculated for each event, on which a cut is then applied. Another set of cosmic-ray simulations can then be used to determine the sensitivity of the analysis. Thereafter, the analysis is applied on the experimental data set. As the current status of the analysis we can report, that we have created a complete template set (explained in detail below). The further steps described above are currently ongoing.

3.2 Complete template set

Before creating the template set, the parameter space needs to be defined. For this work, the parameter space will be 5 dimensional and consists of the following parameters: cosmic-ray zenith angle, azimuth rotation angle of the LPDA, x and y position of the detector relative to the air-shower and $X_{\max}$. The energy dependence of the simulated waveforms was investigated and it was found that the energy mainly changes the amplitude of the signal. The correlation is independent of scaling factors and therefore, the cosmic-ray energy does not need to be taken into account.

In total 85 air-shower simulations for Greenland are picked such that they span a grid over the complete parameter space. The simulations are performed with CORSIKA [13] and the radio emission is calculated with CoREAS [14]. Only proton primaries are used for the simulations, since they cover the widest range of heights of shower maximum. Additionally, all simulations are performed with the same azimuth angle. The magnetic field is very vertical at Summit Station (inclination 81.12°) and therefore, the air showers are expected to have a negligible azimuth angle dependency. Before using the simulations, they are 'denoised', by rejecting simulation artifacts and simulations containing no physical signal.

The signal is short in time and can occur anywhere on the waveform. As a result, a scan of the complete waveform with the template is performed by shifting the waveforms relative to each other. The correlation value is defined as the maximal value of the scan and is calculated with the following formula:

$$\rho = \max\left(\rho(\Delta n)\right) = \max\left(\frac{\sum_i^m (V_1)_i \cdot (V_2)_{i+\Delta n}}{\sqrt{\sum_i^m (V_1)_i^2} \cdot \sqrt{\sum_{j=\Delta n}^{m+\Delta n} (V_2)_j^2}}\right) \tag{1}$$

with V_1 (V_2) being the recorded voltage waveforms of the template (signal), Δn the number of samples by which one waveform is shifted relative to the other and m the length of the template waveform. In order to mitigate the influence of the noise before and after the signal, only a 200 ns window around the maximal amplitude will be used as template.

Check for completeness:

For a template set to cover the parameter space completely, it needs to describe all possible signals in the parameter space. In this analysis, this is the case if the correlation of the template set with all simulations in the parameter space is larger than 0.8. If multiple templates are used, it also needs to be checked that all templates are overlapping each other.

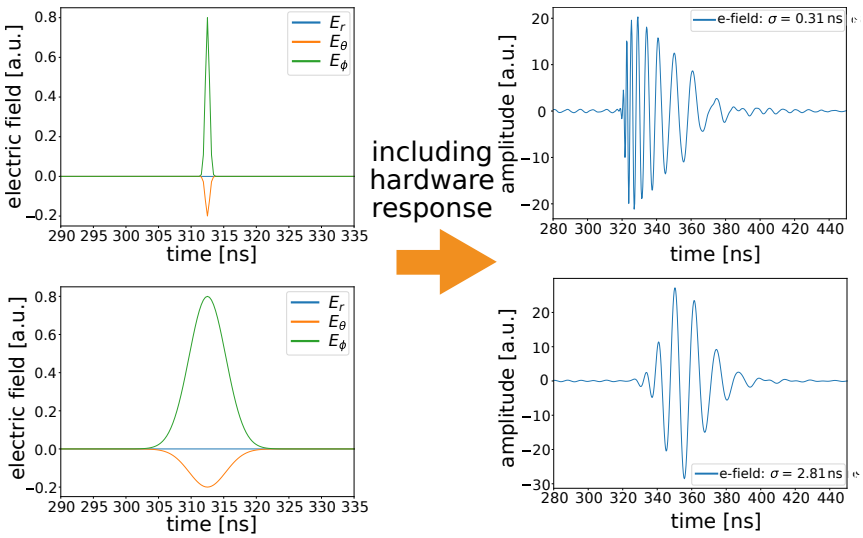

Figure 2: Visualization of the template creation for two different events. The upper plot shows Gaussian functions with a very small width σ = 0.31 ns. The lower plot shows a Gaussian function with a width of σ = 3.13 ns.

Final template set:

As visible in Figure 1b, the air-shower signal is strongly influenced by the hardware response of the detector. Indeed, the main features are created by the hardware response. Therefore, simple Gaussian functions are assumed for the electric field components, except for the component in the direction of propagation (E_r) which is set zero. Two examples of a Gaussian function with a different sample width can be found in Figure 2. Already in this figure, it is visible that the approach is capable of recreating some of the main features of the signal. The influence of different relative amplitudes of the two E-field components was investigated and showed no major influence. As a result, the relative amplitudes are estimated from a single point in parameter space. Two templates with the width of the Gaussian functions of $\sigma_\mathrm{temp1} = 1.56\,\mathrm{ns}$ and $\sigma_\mathrm{temp2} = 1.25\,\mathrm{ns}$ are chosen as a template set. Out of the 55040 simulations spanning the parameter space, only 30 simulation (0.05 %) are not found by the two templates. An investigation of these events showed that they can be excluded from parameter space, because they are either simulations artifacts from close to the shower axis or slipped through the denoising cut. The denoisning cut is constructed conservatively and thus let more simulations through than a realistic trigger would trigger on. In addition, it was shown that each time the template $\sigma_\mathrm{temp1} = 1.56\,\mathrm{ns}$ does not find a simulation, the other template finds it and all its neighboring points in parameter space, thus showing that they overlap. As a result, the two templates are covering the complete parameter space and are a complete template set. The mean correlation score of the template set with all simulations (always choosing the maximal of the two correlations scores) is $\bar{\chi} = 0.89$. To increase the mean correlation score an additional template with a width of $\sigma_\mathrm{temp3} = 0.62\,\mathrm{ns}$ is included, raising the mean correlation score to $\bar{\chi} = 0.94$. Before including the last template, it was checked that the additional template is not increasing the correlation of the template set with noise significantly. A plot showing the three templates can be found in Figure 3.

3.3 Insight into RNO-G data

In the following, an insight into RNO-G data is provided by showing the results of the template matching with some data of station 22 (deployed in 2021) and station 13 (deployed in 2022). The

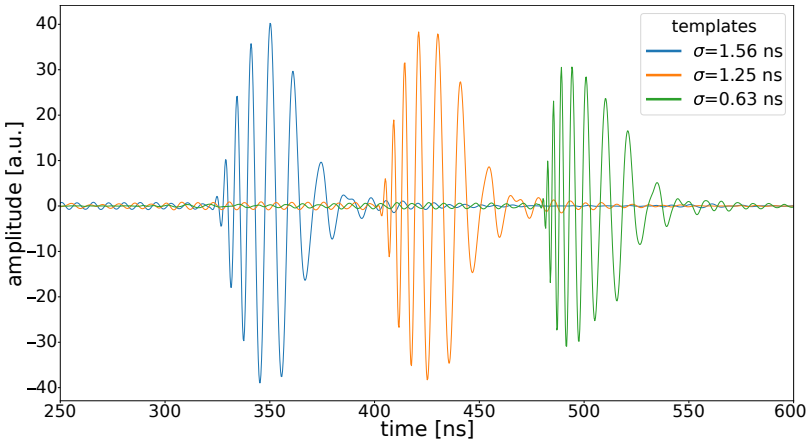

Figure 3: The plot shows the three templates used in the final template set. The Gaussian functions of the templates have a width of σ = 1.56, 1.25, 0.62 ns going from left to right.

sample used is the data sent to DESY in real-time via satellite, which is randomly selected ~ 3% of the total data. In addition, only events triggered by the LPDAs (radiant trigger) or a software trigger (forced trigger) are selected. For the time period, August 3rd till the August 10th 2022 is chosen. In Figure 4 a plot for each station with the correlation value plotted against the trigger time can be found. The plot shows some time clustered features. For example, in both plots, there are spikes going to smaller correlation value (see e.g. 2022/08/04). The corresponding events show a continuous wave with most of them having a frequency of 403 Hz, which can be related to a weather balloon released at Summit Station. In addition, the noise from the solar panels, charging the batteries can be seen as a strong day night variations in the plot of station 22. This specific kind of noise was mitigated for the new stations by redesigning the charging system of the stations. Sometimes there are correlation spikes going to higher correlation values (see e.g. plot of station 13). These events are harder to relate to a specific source, but a potential origin is e.g. a snowmobile passing by. Cosmic rays are not time clustered and can be excluded as origin of the events in the spikes. Further, the rate of UHECR at energies RNO-G is expected to be sensitive is low, only a few UHECR per day in the complete array of 35 station.

A plot showing the correlation plotted against the signal-over-noise-ratio (SNR), for the two example stations, is shown in Figure 5. The SNR is defined as the maximal amplitude A of the signal divided by the voltage RMS (V_{RMS}) of the noise (SNR = $\frac{A}{V_{RMS}}$). The V_{RMS} of the noise is calculated by selecting 100 random events with a forced trigger and calculating the mean RMS for each channel. From simulation cosmic-ray events are expected to populate the region above the red lines shown in Figure 5. The line indicates where the expected cosmic-ray region starts. It was created by estimating the template-signal correlation behavior for small SNR, by adding noise with different amplitudes to a small set of cosmic-ray simulations and then calculating the correlation with the template set. For high SNR the line is set to a correlation value of 0.8 (boundary used to show that the template set is complete). A precise study of the expected cosmic-ray event distribution is still work in progress. In conclusion, for both station there is no major leakage of noise into the cosmic-ray region, making it very likely that this analysis will work for the RNO-G experiment.

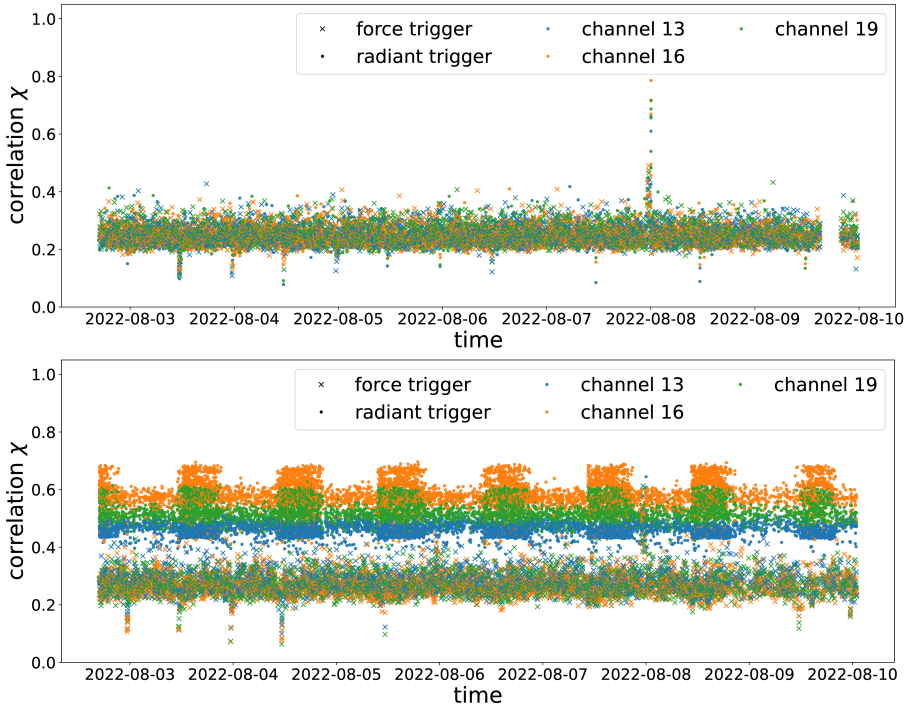

Figure 4: Correlation vs time for the data in the time period of August 3rd till the August 10th 2022. The upper plot shows the result for station 13 and and the lower plot shows the result for station 22. The forced trigger is a software trigger taken very 10 seconds and the radiant trigger is triggering on the signals from the LPDAs.

4. Conclusion

In conclusion, we have presented the general plan of an analysis to find cosmic-ray induced air showers with the Radio Neutrino Observatory - Greenland (RNO-G). In more detail, we presented a method to find a set of templates covering the complete parameter space. With this method we are able to find a complete template set which only contains two templates. By adding a third template, the overall correlation score can be increased. Additionally, we gave an insight into the analysis by showing the application of the template set to 8 days of data for two stations. It was shown that no major leakage of noise is visible into the region of interest. Thus the presented method is very promising for RNO-G. For the future, it is planned to study the expected cosmic-ray event distribution and to analyze more data to find the first cosmic-ray events with RNO-G.

References

[1] RNO-G collaboration, J. A. Aguilar et al., *Design and Sensitivity of the Radio Neutrino Observatory in Greenland (RNO-G)*, *JINST* **16** (2021) P03025, [2010.12279].

[2] IceCube-Gen2 collaboration, M. G. Aartsen et al., *IceCube-Gen2: the window to the extreme Universe*, *J. Phys. G* **48** (2021) 060501, [2008.04323].

[3] G. A. Askar'yan, *Excess negative charge of an electron-photon shower and its coherent radio emission*, *Zh. Eksp. Teor. Fiz.* **41** (1961) 616–618.

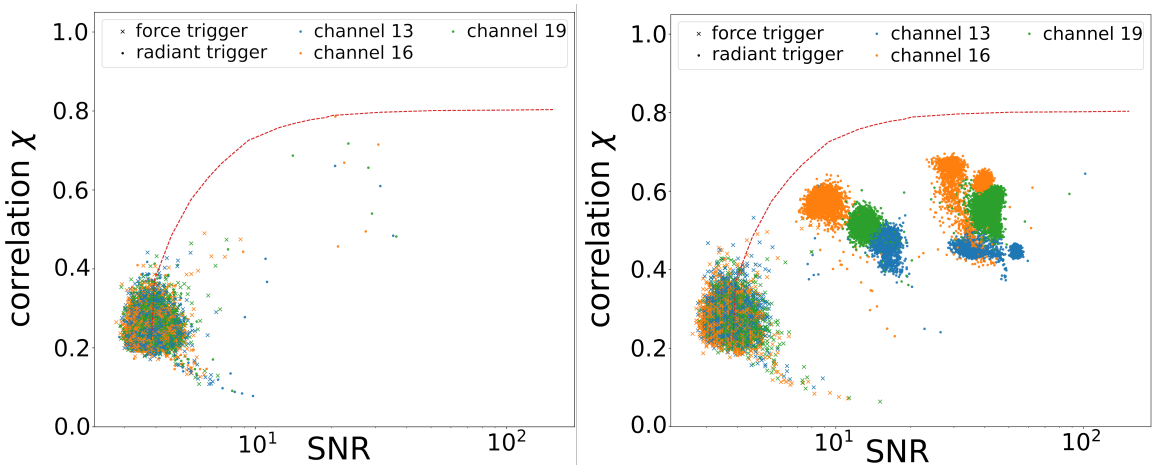

Figure 5: Correlation as function of SNR plotted for the data in the period of August 3rd till the August 10th 2022. The left plot shows the result for station 13 and the right plot for station 22. In both plots, a big blob of data at small SNR and small correlation values is visible, which is mainly populated by the forced trigger events. The tail, going from the blob to lower correlation values and higher SNR, comes from the continuous waves events. Station 22 shows two more event populations. The one at smaller SNR values can be attributed to noise from LoRaWAN (Long Range Wide Area Network used for station communication) and the one at higher SNR values comes from the charging noise. For station 13, it was possible to mitigate both noise sources.

[4] RNO-G collaboration, I. Plaisier et al., *Direction Reconstruction for the Radio Neutrino Observatory Greenland (RNO-G)*, *PoS* **ICRC2021** (2021) 1026.

[5] J. A. Aguilar et al., *Reconstructing the neutrino energy for in-ice radio detectors: A study for the Radio Neutrino Observatory Greenland (RNO-G)*, *Eur. Phys. J. C* **82** (2022) 147.

[6] J. Aguilar et al., *Triboelectric backgrounds to radio-based polar ultra-high energy neutrino (uhen) experiments*, *Astroparticle Physics* **145** (2023) 102790.

[7] O. Scholten, K. Werner and F. Rusydi, *A macroscopic description of coherent geo-magnetic radiation from cosmic-ray air showers*, *Astroparticle Physics* **29** (2008) 94–103.

[8] F. D. Kahn and I. Lerche, *Radiation from cosmic ray air showers*, *Proc. R. Soc. Lond. A* **289** (1966) 206–213.

[9] L. Pyras and I. Plaisier for the RNO-G collaboration, *The radio neutrino observatory greenland: Status update and prospect for air showers*, *PoS* **ECRS** (2022) 088.

[10] S. D. Kockere, K. de Vries, N. van Eijndhoven and U. Latif, *Simulation of in-ice cosmic ray air shower induced particle cascades*, *Physical Review D* **106** (2022) 043023.

[11] R. Rice-Smith, *Assessing the Background Rate due to Cosmic Ray Core Scattering from Internal Reflection Layers in the South Pole Ice Cap*, July, 2022. 10.5281/zenodo.6785120.

[12] S. W. Barwick et al., *Radio detection of air showers with the ARIANNA experiment on the Ross Ice Shelf*, *Astropart. Phys.* **90** (2017) 50–68, [1612.04473].

[13] D. Heck, J. Knapp, J. N. Capdevielle, G. Schatz and T. Thouw, *CORSIKA: A Monte Carlo code to simulate extensive air showers*, *Wissenschaftliche Berichte* **FZKA-6019** (1998) 1–90.

[14] T. Huege, M. Ludwig and C. W. James, *Simulating radio emission from air showers with coreas*, *AIP Conference Proceedings* **1535** (2013) 128–132.

Full Author List: RNO-G Collaboration

J. A. Aguilar[1], P. Allison[2], D. Besson[3], A. Bishop[4], O. Botner[5], S. Bouma[6], S. Buitink[7], M. Cataldo[6], B. A. Clark[8], K. Couberly[3], Z. Curtis-Ginsberg[9], P. Dasgupta[1], S. de Kockere[10], K. D. de Vries[10], C. Deaconu[9], M. A. DuVernois[4], A. Eimer[6], C. Glaser[5], A. Hallgren[5], S. Hallmann[11], J. C. Hanson[12], B. Hendricks[13], J. Henrichs[11,6], N. Heyer[5], C. Hornhuber[3], K. Hughes[9], T. Karg[11], A. Karle[4], J. L. Kelley[4], M. Korntheuer[1], M. Kowalski[11,14], I. Kravchenko[15], R. Krebs[13], R. Lahmann[6], U. Latif[10], J. Mammo[15], M. J. Marsee[16], Z. S. Meyers[11,6], K. Michaels[9], K. Mulrey[17], M. Muzio[13], A. Nelles[11,6], A. Novikov[18], A. Nozdrina[3], E. Oberla[9], B. Oeyen[19], I. Plaisier[6,11], N. Punsuebsay[18], L. Pyras[11,6], D. Ryckbosch[19], O. Scholten[10,20], D. Seckel[18], M. F. H. Seikh[3], D. Smith[9], J. Stoffels[10], D. Southall[9], K. Terveer[6], S. Toscano[1], D. Tosi[4], D. J. Van Den Broeck[10,7], N. van Eijndhoven[10], A. G. Vieregg[9], J. Z. Vischer[6], C. Welling[9], D. R. Williams[16], S. Wissel[13], R. Young[3], A. Zink[6]

[1]ULB Brussels, Université Libre de Bruxelles, Science Faculty CP230, B-1050 Brussels, Belgium
[2]Ohio State University, Dept. of Physics, Center for Cosmology and AstroParticle Physics, Ohio State University, Columbus, OH 43210, USA
[3]University of Kansas, University of Kansas, Dept. of Physics and Astronomy, Lawrence, KS 66045, USA
[4]University of Wisconsin-Madison, Wisconsin IceCube Particle Astrophysics Center (WIPAC) and Dept. of Physics, University of Wisconsin-Madison, Madison, WI 53703, USA
[5]Uppsala University, Uppsala University, Dept. of Physics and Astronomy, Uppsala, SE-752 37, Sweden
[6]Friedrich-Alexander-University Erlangen-Nürnberg, Erlangen Center for Astroparticle Physics (ECAP), Friedrich-Alexander-University Erlangen-Nürnberg, 91058 Erlangen, Germany
[7]VUB Brussels, Vrije Universiteit Brussel, Astrophysical Institute, Pleinlaan 2, 1050 Brussels, Belgium
[8]Michigan State University, Dept. of Physics and Astronomy, Michigan State University, East Lansing MI 48824, USA
[9]University of Chicago, Dept. of Physics, Enrico Fermi Inst., Kavli Inst. for Cosmological Physics, University of Chicago, Chicago, IL 60637, USA
[10]Vrije Universiteit Brussel, Vrije Universiteit Brussel, Dienst ELEM, B-1050 Brussels, Belgium
[11]DESY, Deutsches Elektronen-Synchrotron DESY, Platanenallee 6, 15738 Zeuthen, Germany
[12]Whittier College, Whittier College, Whittier, CA 90602, USA
[13]Penn State University, Dept. of Physics, Dept. of Astronomy & Astrophysics, Penn State University, University Park, PA 16801, USA
[14]HU Berlin, Institut für Physik, Humboldt-Universität zu Berlin, 12489 Berlin, Germany
[15]University of Nebraska-Lincoln, Dept. of Physics and Astronomy, Univ. of Nebraska-Lincoln, NE, 68588, USA
[16]University of Alabama, Dept. of Physics and Astronomy, University of Alabama, Tuscaloosa, AL 35487, USA
[17]Radboud University, Dept. of Astrophysics/IMAPP, Radboud University, PO Box 9010, 6500 GL, The Netherlands
[18]University of Delaware, Dept. of Physics and Astronomy, University of Delaware, Newark, DE 19716, USA
[19]Ghent University, Ghent University, Dept. of Physics and Astronomy, B-9000 Gent, Belgium
[20]University of Groningen, Kapteyn Institute, University of Groningen, Groningen, The Netherlands

PoS(ARENA2022)007